Sensors and Materials, Vol. 34, No. 4 (2022) 1617–1626
MYU Tokyo

S & M 2914

Improving Performance of Odor Biosensor System Using Olfactory Receptor

Yasufumi Yokoshiki,[1] Keito Nagayoshi,[2] Hidefumi Mitsuno,[3] Sawako Niki,[3] Ryohei Kanzaki,[3] Takashi Tokuda,[1] and Takamichi Nakamoto[1*]

[1]Institute of Innovative Research, Tokyo Institute of Technology,
2-12-1 Ookayama, Meguro-ku, Tokyo 152-8550, Japan
[2]Department of Electrical and Electronic Engineering, Tokyo Institute of Technology,
2-12-1 Ookayama, Meguro-ku, Tokyo 152-8550, Japan
[3]Research Center for Advanced Science and Technology, The University of Tokyo,
4-6-1 Komaba, Meguro-ku, Tokyo 153-8904, Japan

(Received December 2, 2021; accepted March 9, 2022)

Keywords: odor biosensor, cell-based sensor, olfactory receptor, odor detection system

Odor sensors based on olfactory receptors, which have high sensitivity and selectivity, have attracted much attention in recent years. We previously reported on the quantification of binary gas mixtures. To increase the number of components and the resolution of our odor biosensor system, it is necessary to improve the reproducibility and reduce the sensor response time. In this study, we examined the parameters related to the reproducibility and response time, such as the volume of liquid in the chamber channel, the flow rate of the buffer solution, and the pressure of the micro-dispenser, to improve the performance of the system. It was found that the response time was shortened by reducing the volume of liquid in the chamber and increasing the flow rate. It was also found that stable injection was achieved by adjusting the pressure applied to the micro-dispenser as a function of the drive frequency. We reduced the average response time of our system from 160 to 57 s. Moreover, we avoided an increase in the injection volume and droplet generation by applying appropriate pressures to the micro-dispenser.

1. Introduction

An odor is a gas mixture composed of several volatile compounds. For gas analysis, semiconductor gas sensors,[1] a quartz crystal microbalance,[2,3] surface plasmon resonance,[4] surface acoustic waves,[5] gas chromatography–mass spectrometry,[6,7] and field asymmetric ion mobility spectrometry[8,9] are generally utilized. Recently, research on odor biosensors has attracted much attention because olfactory receptors have high potential due to their high sensitivity and selectivity. Insect olfactory receptors (ORs) are promising for sensor applications because they have ion channels composed of ORs and olfactory receptor co-receptors (ORCOs), although mammals have G-protein coupled receptors (GPCRs). Therefore, these ORs can be used as a sensor by expressing fluorescent proteins into cells to obtain a fluorescence response.

*Corresponding author: e-mail: nakamoto.t.ab@m.titech.ac.jp
https://doi.org/10.18494/SAM3765

ISSN 0914-4935
https://myukk.org/

We previously reported a system that measures the response of cells to odors by measuring the fluorescence response with an image sensor.[10]

As an application of the E-nose, we studied a device that records and reproduces odors.[11–13] This device was based on mixing primary odors to create a similar odor to the target odor. Sensors with ORs are promising for use in devices because it is essential to discriminate different concentrations of gas mixtures. We previously reported binary gas mixture quantification with ORs.[14] To extend our system, its performance must be improved, such as its response time and reproducibility. In our previous work, the average response time was 160 s, which is too long to enable the use of an algorithm for quantification. Other problems with the system were fluctuation of the injection volume and occasional injection failure due to droplet formation. Here, we report the results of optimizing the parameters of the system, such as the flow rate of buffer solution, the volume of liquid in the chamber, and the back pressure applied to the micro-dispenser.

2. Materials and Methods

In this study, Or49b ORs were used. As shown in Fig. 1(a), they were transduced and functionally expressed together with ORCOs on the membrane of Sf21 cells derived from *Spodoptera frugiperda*.[15–17] GCaMP6s[18] was used as a calcium-sensitive protein to obtain a fluorescence response to calcium ions in the cells.

Cells were attached to the bottom of a polydimethylsiloxane (PDMS) channel filled with buffer solution in the measurement system [Fig. 1(b)]. The composition of the buffer solution has been reported elsewhere.[17] The buffer solution was replaced using a syringe pump (Legato 111, kdScientific) at a constant flow rate (100 or 500 μL/s) to preserve the condition of the cells. The solution was injected and removed at the same flow rate from the inlet and outlet of the flow path using syringe pumps to avoid changing the volume of solution in the flow path. We cultured the cells in a 25 cm^2 flask, and we used the cells two days after the start of cell culture. We injected 2.0 mL of buffer solution and 0.1% DMSO after washing the inside of the flask with the same solution. After that, 25 μL of the buffer solution with cells was injected into the PDMS

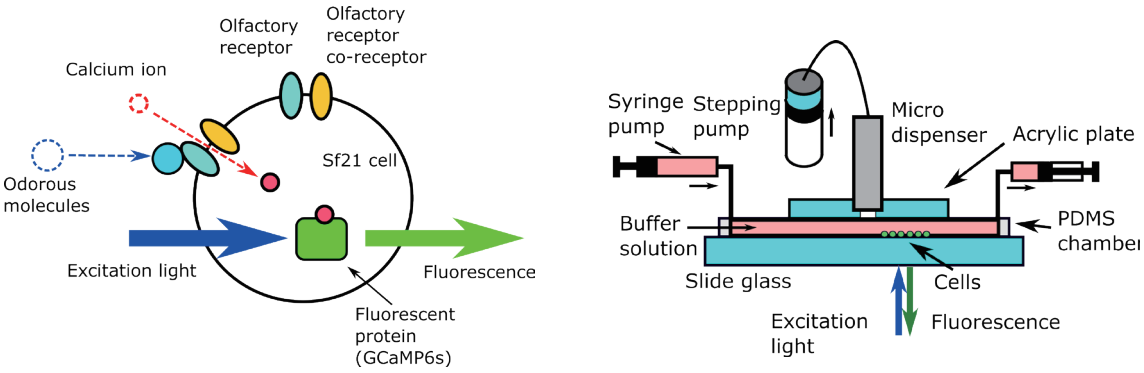

(a) (b)

Fig. 1. (Color online) Odor detection system. (a) Mechanism of odor detection using cells and (b) schematic diagram of the odor measurement system.

flow path and left for 10 min to attach the cells to the bottom surface. The procedure was performed again if the number of cells measured by an image sensor was not in the range of 200–400 cells. The cell response was measured by emitting excitation light from a 25 mW laser diode module (wavelength: 488 nm), separating the excitation light using a dichroic mirror, and then recording the fluorescence intensity using an image sensor.[14] The average fluorescence intensity of all cells in images was used as the response. A micro-dispenser (INKA2438510H, Lee Company) capable of injecting a small number of droplets was used to inject the odor. The stimulation time was 5 s. The odor (800 μM *o*-cresol) was dissolved in buffer solution mixed with 0.1% DMSO solution. The odor solution was supplied using a micro-dispenser and the injection volume was controlled by changing the frequency of the applied voltage. Droplets easily formed, as described in Sect. 2.3, because of the viscosity of the odor solution. Therefore, a constant pressure was applied using a stepping pump to prevent problems with the injection.

2.1 Relationship between flow rate and response change

In this study, the buffer solution was flowed into the chamber at a constant flow rate using a syringe pump to avoid odor stagnation and to refresh cells. The structure of the flow path is shown in Fig. 2(a). The cells were attached to the bottom surface, as shown in Fig. 2(b). The odor was mixed with the buffer solution in the chamber and reached the cells. The flow rate could be increased by changing the speed of the syringe pump used to eject the buffer solution. The odor was expected to reach the cells quickly and be released rapidly from the ORs when the flow rate was increased, reducing the response time of the odor sensor. In this experiment, we examined flow rates of 100 and 500 μL/s. The driving frequency of the micro-dispenser was 300 Hz and the response was measured three times for each flow rate. The volume of liquid in the flow path was 25 μL and the speed of the stepping pump was 30 steps/s.

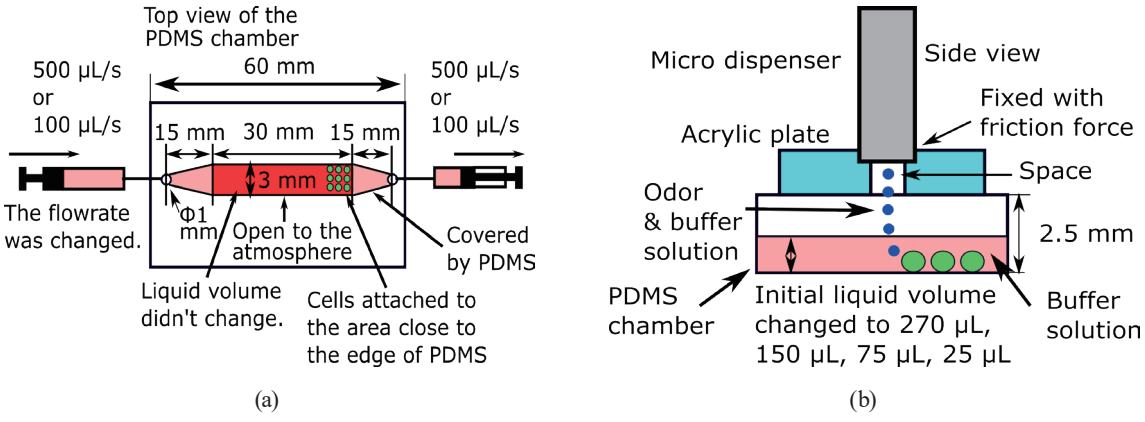

Fig. 2. (Color online) Structure of the flow path. (a) Top view and (b) side view.

2.2 Relationship between volume of liquid in flow path and sensor response

We examined how the odor response changes upon reducing the amount of solution in the flow path. There was no change in the volume of liquid in the flow path since the injection and discharge flow rates were the same as shown in Fig. 2(a). Part of the chamber was open to the atmosphere to enable the injection of odor. Therefore, the initial volume of liquid in the flow path was changed using a syringe, as shown in Fig. 2(b). The examined volumes of liquid were 270, 150, 75, and 25 μL. The flow rate was 100 μL/s and the driving frequency of the micro-dispenser was 100 Hz. The response was measured three times for each volume. The speed of the stepping pump was 10 steps/s.

2.3 Stabilizing the injection volume of micro-dispenser

If no pressure is applied when a viscous liquid such as a buffer solution is injected from a micro-dispenser, then injected small droplets sometimes adhere to the orifice [Fig. 3(a)] and may grow [Fig. 3(b)]. If liquid accumulates around the orifice, then it is not ejected. As a result, the odor does not reach the cells.

Furthermore, pressure control was necessary for the injection of odors by the micro-dispenser. A stepping pump (LPDA2720125D, Lee Company) was used to ensure that the exact amount of liquid was injected to the inlet of the micro-dispenser. For reproducibility, it is necessary to inject the liquid at an appropriate pressure because the injection volume depends on the pressure in the micro-dispenser. In this experiment, we used stepping pump speeds of 5, 10, and 20 steps/s. A stepping motor drove the stepping pump, and we used a 1/128 micro-step to increase the resolution of the motor. Since the injection volume at the full step was 0.2 μL, the injection volume at the micro-step was 0.2/128 μL. Therefore, the volume conversions were about 7.8, 15.6, and 31.2 nL/s for the stepping pump speeds of 5, 10, and 20 steps/s, respectively. The volume of liquid in the flow path was 25 μL.

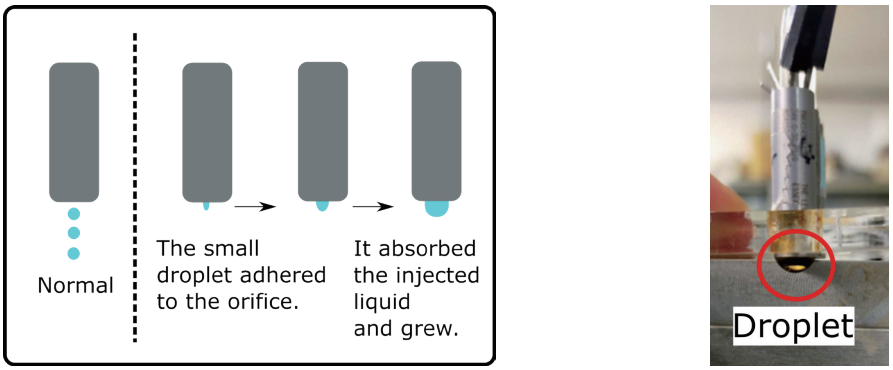

(a) (b)

Fig. 3. (Color online) Storage of droplet in apertures. (a) Growth mechanism and (b) image of droplet.

3. Results and Discussion

3.1 Relationship between flow rate and response change rate

The results of the experiment when the flow rate was changed are shown in Fig. 4. The rising time was the time from the odor injection to the maximum response [Fig. 4(a)], and the falling time was the time from the maximum response to the baseline [Fig. 4(b)]. The sum of these two values was the odor response time [Fig. 4(c)]. A typical sensor response is shown in Fig. 4(d). We considered that the response had returned to the baseline when the change in the response became sufficiently small (a value of 0.01 was set for a peak value of approximately 50) since the baseline fluctuated. The average response time at a flow rate of 100 µL/s and a buffer volume of 150 µL was 160 s in our previous work.

A paired *t*-test was performed on these results, and significant differences were found in all cases (a *p*-value of less than 0.050 was considered statistically significant). The *p*-values of the rising, falling, and response times were 0.0059, 0.044, and 0.026, respectively. The reason for the rapid rising time is considered to be that the time for the odor to reach the cells was reduced at a higher flow rate. In addition, the time for the odor to leave the cells was also shorter. This may be due to the fact that more buffer solution reaches the cells per unit of time, accelerating the release of the odor. From this experiment, we confirmed that the flow rate is a parameter determining the response speed and that the response time of the odor can be shortened by increasing the flow rate.

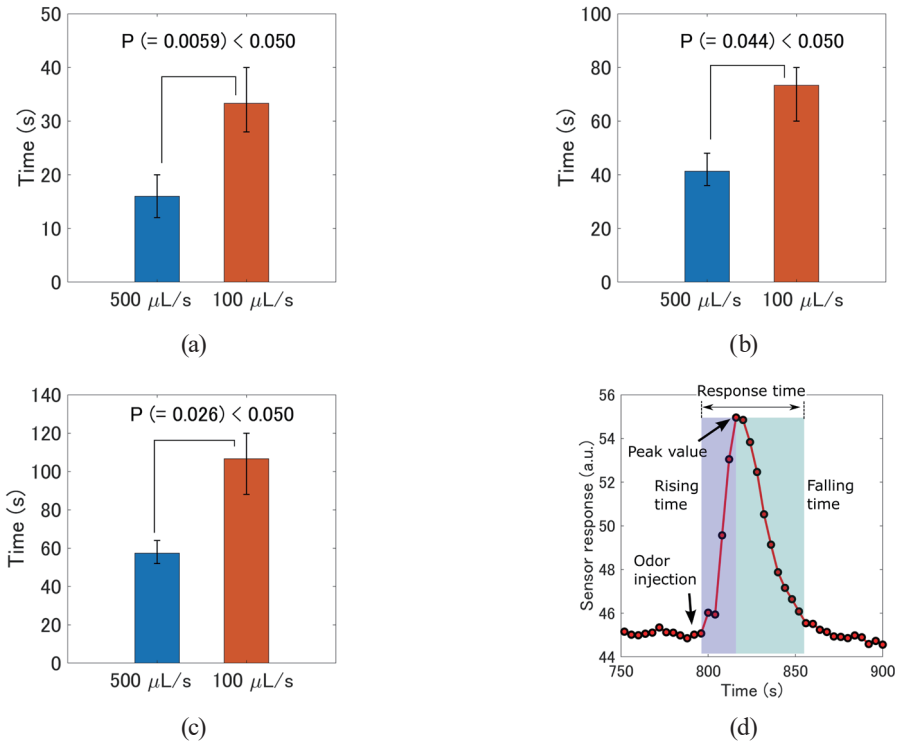

Fig. 4. (Color online) Rising and falling times when the flow rate was changed. (a) Rising time, (b) falling time, (c) response time, and (d) example of typical sensor response.

3.2 Relationship between volume of liquid in flow path and sensor response

When the volume of liquid was 270 μL, which is the maximum capacity of the flow channel, no response was observed. Figure 5 shows the measurement results for liquid volumes of 150, 75, and 25 μL. The peak response value [Fig. 5(a)] and rising time [Fig. 5(b)] were significantly different ($p < 0.5$) for liquid volumes of 150 and 75 μL according to the paired *t*-test, with *p*-values of 0.014 and 0.017, respectively. There was no significant difference between the results for volumes of 75 and 25 μL (*p*-values of 0.075 and 0.42, respectively). The lack of response for the liquid volume of 270 μL was considered to be due to the excessive volume of the solution diluting the odor to below the detection limit in the flow path. The results indicate that there was a threshold level in the range of 75–150 μL at which most of the odor reaches the cells. Therefore, the difference between the results for liquid volumes of 75 and 25 μL was small. The amount of solution in the flow path should be less than 75 μL to ensure a large and fast response.

3.3 Stabilizing the injection volume of micro-dispensers

We examined the pressure applied to the micro-dispenser in the frequency range up to 200 Hz and found that injection was successful at step pumping speeds of 10 or more steps/s. As the driving frequency of the micro-dispenser increases, it becomes more difficult to increase the pressure inside the micro-dispenser and easier for droplets to form. When the micro-dispenser injects a low-viscosity solution (e.g., water), droplets are less likely to form. Therefore, we reduced the viscosity of the buffer solution by performing measurements using odor diluted with pure water. However, the cells did not show any response. This was probably because the calcium ion influx into the cells was reduced when only the diluted odorant was used. Therefore, back pressure control of the micro-dispenser is an important technique.

Furthermore, if the pressure is increased too much, the pressure inside the micro-dispenser will not drop sufficiently after droplet injection, resulting in a variation in the injection volume. We applied different pressures and measured the amount of odor injected from the micro-dispenser to examine the variation in the amount of injection The amount of injection was measured as the mass change of a paper due to liquid injection using an electronic balance.

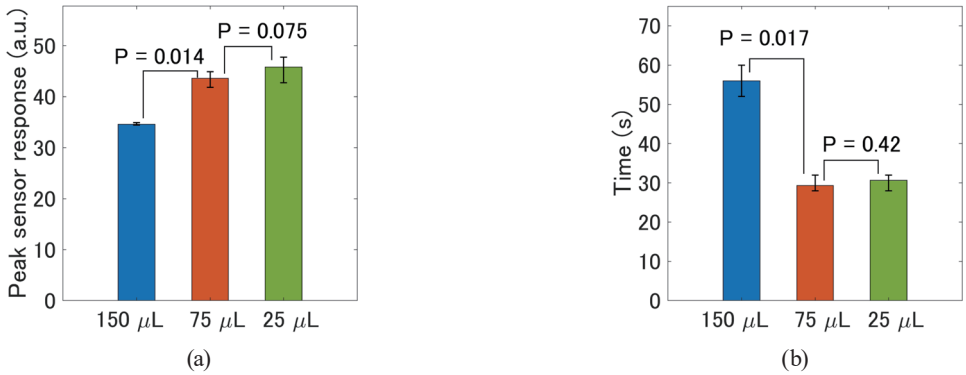

Fig. 5. (Color online) Peak value of sensor response and rising time for different volumes of liquid in the flow path: (a) peak value and (b) rising time.

The amount of injection increased when the pressure was 20 steps/s and the driving frequency was 200 Hz, as shown in Fig. 6(a). According to the results, the pressure inside the micro-dispenser may not decrease entirely due to the injection. On the other hand, the injection volume was stable when the pressure was 5 steps/s and the driving frequency was 30 Hz. This is considered to be because the internal pressure is probably constant because the injection volume from the micro-dispenser and the supplied volume from the stepping pump with the micro-dispenser are balanced. It was found that if the pressure was lowered, the same amount of liquid was injected each time. However, when the pressure was 5 steps/s and the driving frequency was increased, drops were generated when the driving frequency was 200 Hz. This driving frequency had the greatest effect on the next injection volume because it caused the largest pressure fluctuation inside the micro-dispenser due to the high pressure. On the other hand, the injection volume for the driving frequency of 30 Hz was also easily affected by pressure fluctuation because it was difficult to reduce the internal pressure owing to the intermittent small injection volume (when the injection volume of the micro-dispenser does not equal the supplied volume from the stepping pump with the micro-dispenser, the pressure inside the micro-dispenser fluctuates). We selected the most difficult conditions: driving frequencies of 30 and 200 Hz. These are the most difficult conditions because the micro-dispenser is most sensitive to the generation of droplets at a driving frequency of 200 Hz and most affected by the pressure inside the micro-dispenser at a driving frequency of 30 Hz. Figure 6(b) shows the injection volume when the odor was injected alternately at 200 and 30 Hz. The step pumping speeds were set to 10 steps/s at 200 Hz and to 5 steps/s at 30 Hz. The results show that the injection volume was stable at both frequencies. Also, no droplets were formed during the experiment. This indicates that the injection volume of the micro-dispenser can be stabilized by adjusting the pressure according to the driving frequency.

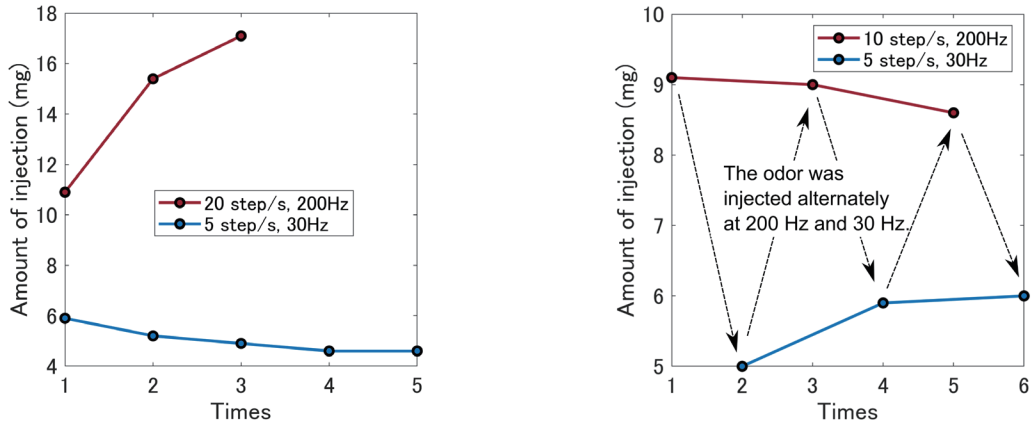

Fig. 6. (Color online) Amount of injection when pressure changed: (a) unstable injection volume (20 steps/s, 200 Hz) and stabilized volume (5 steps/s, 30 Hz) and (b) improvement of the reproducibility using different pressures.

4. Conclusions

We examined how changes in parameters affect the sensor response and stabilize the injection volume of a micro-dispenser in an odor biosensor system using an olfactory receptor. Our experiments showed that the response time was shortened by increasing the flow rate and decreasing the volume of liquid in the flow path. We reduced the average response time approximately threefold from 160 s in our previous study to 57 s, making it possible to use a concentration quantification algorithm that requires multi-point measurement and an odor identification algorithm. The reduced response time is effective from the viewpoint of application. In our previous work, the injection volume increased by around 6 mg at 200 Hz within three continuous injections, becoming around 1.5 times the initial injection volume. Moreover, the injection occasionally failed due to droplet formation. We avoided such an increase in the injection volume and droplet formation by applying appropriate pressures to the micro-dispenser. We showed that the internal pressure of the micro-dispenser is an essential parameter determining the droplet ejection volume and that it is necessary to adjust the pressure to improve reproducibility. We plan to use the results of this study for research on multi-component quantification in the future.

References

1 H. Araki, M. Oura, and S. Omatu: Artif. Life Robot. **23** (2018) 1. https://doi.org/10.1007/s10015-017-0403-0
2 B. P. Regmi, P. L. Adhikari, and B. B. Dangi: Chemosensors **9** (2021) 194. https://doi.org/10.3390/chemosensors9080194
3 M. Aleixandre and T. Nakamoto: Sensors **20** (2020) 4026. https://doi.org/10.3390/s20144026
4 T. Onodera and K. Toko: Sensors **14** (2014) 16586. https://doi.org/10.3390/s140916586
5 T. Nakamoto, K. Aoki, T. Ogi, S. Akao, and N. Nakaso: Sens. Actuators, B **130** (2008) 386. https://doi.org/10.1016/j.snb.2007.09.022
6 M. Aznar, R. López, J. F. Cacho, and V. Ferreira: J. Agric. Food Chem. **49** (2001) 2924. https://doi.org/10.1021/jf001372u
7 D. Prasetyawan and T. Nakamoto: IEEE Access **9** (2021) 134402. https://doi.org/10.1109/ACCESS.2021.3115760
8 Y. Yokoshiki and T. Nakamoto: Sensors **19** (2019) 3007. https://doi.org/10.3390/s19133007
9 J. A. Covington, M. P. van der Schee, A. S. L. Edge, B. Boyle, R. S. Savage, and R. P. Arasaradnam: Analyst **140** (2015) 6775. https://doi.org/10.1039/C5AN00868A
10 T. Mujiono, Y. Sukekawa, T. Nakamoto, H. Mitsuno, M. Termtanasombat, R. kanzaki, and N. Misawa: Sens. Mater. **29** (2017) 65. https://doi.org/10.18494/SAM.2017.1378
11 T. Yamanaka, R. Matsumoto, and T. Nakamoto: Sens. Actuators, B **87** (2002) 457. https://doi.org/10.1016/S0925-4005(02)00300-3
12 T. Yamanaka, R. Matsumoto, and T. Nakamoto, Sens. Actuators, B **89** (2003) 112. https://doi.org/10.1016/S0925-4005(02)00451-3
13 Y. Yokoshiki and T. Nakamoto: Sensors **19** (2019) 5442. https://doi.org/10.3390/s19245442
14 Y. Sukekawa, H. Mitsuno, R. Kanzaki, and T. Nakamoto: Biosens. Bioelectron. **179** (2021) 113053. https://doi.org/10.1016/j.bios.2021.113053
15 H. Mitsuno, S. Niki, E. Kuroda, S. Araki, D. Terutsuki, T. Sakurai, and R. Kanzaki: 2019 IEEE Int. Symp. Olfaction and Electronic Nose (IEEE, 2019) 1–3.
16 M. Termtanasombat, H. Mitsuno, N. Misawa, S. Yamahira, T. Sakurai, S. Yamaguchi, T. Nagamune, and R. Kanzaki: J. Chem. Ecol. **42** (2016) 716. https://doi.org/10.1007/s10886-016-0726-7
17 H. Mitsuno, T. Sakurai, S. Namiki, H. Mitsuhashi, and R. Kanzaki: Biosens. Bioelectron. **65** (2015) 287. https://doi.org/10.1016/j.bios.2014.10.026
18 T. W. Chen, T. J. Wardill, Y. Sun, S. R. Pulver, S. L. Renninger, A. Baohan, E. R. Schreiter, R. A. Kerr, M. B. Orger, V. Jayaraman, L. L. Looger, K. Svoboda, and D. S. Kim: Nature **499** (2013) 295. https://doi.org/10.1038/nature12354

About the Authors

Yasufumi Yokoshiki received his D.Eng. degree from Tokyo Institute of Technology, Japan, in 2020. He worked as a postdoctoral researcher after graduation. Since 2020, he has been an assistant professor at the Institute of Innovative Research (IIR), Tokyo Institute of Technology. His research interests are biosensors, odor sensing, digital circuits, machine learning, and energy harvesting. (yokoshiki@ee.e.titech.ac.jp)

Keito Nagayoshi received his B.E. degree from Tokyo Institute of Technology, Japan, in 2019. He is currently pursuing his M.E. degree in electrical and electronic engineering at Tokyo Institute of Technology. (nagayoshi.k.aa@m.titech.ac.jp)

Hidefumi Mitsuno received his Ph.D. degree from Kyoto University, Japan, in 2009. From 2007 to 2020, he was successively a project researcher, a project research associate, and a research associate at the Research Center for Advanced Science and Technology (RCAST), The University of Tokyo, Tokyo, Japan. Since 2020, he has been a project associate professor at RCAST. His research interests are molecular biology, insect physiology, and biosensors. (mitsuno@brain.imi.i.u-tokyo.ac.jp)

Sawako Niki received her M.Sc. degree in science from the Graduate School of Biological Sciences, University of Tsukuba, Japan, in 1994. From 2009 to 2010, she was a technical assistant with the Science Integration Program, Organization for Interdisciplinary Research Projects, The University of Tokyo, Chiba, Japan. From 2011 to 2015, she was a technical assistant with the Department of Complexity Science and Engineering, Graduate School of Frontier Sciences, The University of Tokyo, Chiba, Japan. Since 2016, she has been a project academic support specialist with the Research Center for Advanced Science and Technology (RCAST), The University of Tokyo, Tokyo, Japan. Her research interests are in neurophysiology, ethology, and molecular biology. (niki@brain.imi.i.u-tokyo.ac.jp)

Ryohei Kanzaki received his D.Sc. degree in neurobiology from the Institute of Biological Sciences, University of Tsukuba in 1986. From 1987 to 1990, he was a postdoctoral research fellow at Arizona Research Laboratories, Division of Neurobiology, University of Arizona. From 1991 to 2003, he was successively an assistant professor, an associate professor, and a full professor at the Institute of Biological Sciences, University of Tsukuba. From 2004 to 2006, he was a full professor at the Department of Mechano-Informatics, Graduate School of Information Science and Technology, The University of Tokyo. Since 2006, he has been a full professor at the Research Center for Advanced Science and Technology (RCAST), The University of Tokyo. Since 2016, he has been the director of RCAST. His research interests are in neurophysiology, neuroethology, and biohybrid systems. (kanzaki@rcast.u-tokyo.ac.jp)

Takashi Tokuda received his B.E. and M.E. degrees in electronic engineering and his Ph.D. degree in materials engineering from Kyoto University, Kyoto, Japan, in 1993, 1995, and 1998, respectively. From 1999 to 2008 and from 2008 to 2019, he was an assistant professor with the Graduate School of Materials Science and Nara Institute of Science and Technology (NAIST), respectively. Since 2019, he has been a professor at Tokyo Institute of Technology. His research interests include CMOS image sensors, implantable devices, wireless technology, and IoT. (tokuda@ee.e.titech.ac.jp)

Takamichi Nakamoto received his B.E. and M.E. degrees in 1982 and 1984, respectively, and his Ph.D. degree in electrical and electronic engineering from Tokyo Institute of Technology, Tokyo, Japan. He worked for Hitachi in the area of VLSI design automation from 1984 to 1987. In 1987, he joined Tokyo Institute of Technology as a research associate. In 1993, he became an associate professor with the Department of Electrical and Electronics Engineering, Tokyo Institute of Technology. From 1996 to 1997, he was a visiting scientist at Pacific Northwest Laboratories, Richland, WA, USA. He is currently a professor with the Institute of Innovative Research, Tokyo Institute of Technology. (nakamoto.t.ab@m.titech.ac.jp)